

State-Dependent Cross-Linking of the M2 and M3 Segments: Functional Basis for the Alignment of GABA_A and Acetylcholine Receptor M3 Segments

Michaela Jansen and Myles H. Akabas

Departments of Physiology and Biophysics and of Neuroscience, Albert Einstein College of Medicine of Yeshiva University, Bronx, New York 10461

Construction of a GABA_A receptor homology model based on the acetylcholine (ACh) receptor structure is complicated by the low sequence similarity between GABA_A and ACh M3 transmembrane segments that creates significant uncertainty in their alignment. We determined the orientation of the GABA_A M2 and M3 transmembrane segments using disulfide cross-linking. The M2 residues α 1M266 (11') and α 1T267 (12') were mutated to cysteine in either wild type or single M3 cysteine mutant (α 1V297C, α 1A300C to α 1A305C) backgrounds. We assayed spontaneous and induced disulfide bond formation. Reduction with DTT significantly potentiated GABA-induced currents in α 1T267C-L301C and α 1T267C-F304C. Copper phenanthroline-induced oxidation inhibited GABA-induced currents in these mutants and in α 1T267C-A305C. Intrасubunit disulfide bonds formed between these Cys pairs, implying that the α -carbon separation was at most 5.6 Å. The reactive α 1M3 residues (L301, F304, A305) lie on the same face of an α -helix. The unresponsive ones (A300, I302, E303) lie on the opposite face. In the resting state, the reactive side of α 1M3 faces M2- α 1T267. In conjunction with the ACh structure, our data indicate that alignment of GABA_A and ACh M3 requires a single gap in the GABA_A M2–M3 loop. In the presence of GABA, oxidation of α 1T267C-L301C and α 1T267C-F304C had no effect, but oxidation of α 1T267C-A305C caused a significant increase in spontaneous channel opening. We infer that, as the channel opens, the distance and/or orientation between M2- α 1T267 and M3- α 1A305 changes such that the disulfide bond stabilizes the open state. This begins to define the conformational motion that M2 undergoes during channel opening.

Key words: GABA_A receptor; ion channel; acetylcholine receptor; disulfide cross-linking; glycine; serotonin

Introduction

GABA_A receptors are members of the Cys-loop receptor superfamily of neurotransmitter-gated ion channels that includes acetylcholine, glycine, and 5-HT₃ receptors (Hevers and Lüddens, 1998; Karlin, 2002; Lester et al., 2004). Many general anesthetics and drugs used to treat anxiety, epilepsy, and sleep disorders target GABA_A receptors, which mediate fast inhibitory synaptic transmission. Five homologous subunits, each with an extracellular N-terminal ligand-binding domain and four α -helical transmembrane segments (M1–M4), assemble around the central channel axis to form the receptors. The channel is lined by the five M2 segments, which are surrounded by an outer ring of helices, formed by the M1, M3, and M4 segments (Xu and Akabas, 1996; Miyazawa et al., 2003).

Recently, GABA_A receptor homology models (Cromer et al., 2002; Trudell and Bertaccini, 2004; Ernst et al., 2005) were con-

structed based on the acetylcholine binding protein and *Torpedo* ACh receptor structures (Brejc et al., 2001; Miyazawa et al., 2003; Celie et al., 2004; Unwin, 2005). Homology models depend on the correct alignment of subunit sequences from different superfamily members. Uncertainty in sequence alignment limits the veracity of models. Alignment of ACh and GABA_A M1 and M2 transmembrane segments is facilitated by highly conserved residues corresponding to GABA_A α 1R221, α 1P233, α 1F245, α 1R255, α 1L264, and α 1P278 (Fig. 1) (Le Novère and Changeux, 1999; Ernst et al., 2005). M3 segment alignment is more complicated, because they are mostly hydrophobic with very limited sequence identity (Fig. 1). Thus, multiple sequence alignment programs introduce a variable number of gaps in the GABA_A M2–M3 loop relative to the ACh receptor depending on the number of sequences and the specific subunits that are aligned. Progress in generating correct homology models requires an experimental determination of both the face of the GABA_A M3 segment that interacts with M2 and the vertical position of M3 relative to defined levels in M2. Having the correct structural model is essential to understanding the molecular basis for general anesthetic and alcohol action on GABA_A receptors.

In the current work, we determined the proximity of M2 and M3 residues using disulfide cross-linking between pairs of engineered cysteines. We used two M2 positions, α 1M266 (11') and α 1T267 (12'), that we showed lie opposite to the M2 channel-

Received Jan. 17, 2006; revised March 20, 2006; accepted March 20, 2006.

This work was supported in part by National Institutes of Health Grants NS30808 and GM77660 (M.H.A.). M.J. was supported in part by a fellowship from the Deutsche Forschungsgemeinschaft. We thank Moez Bali, David Liebelt, Nicole McKinnon, David Reeves, and Paul Riegelhaupt for helpful discussions and also for comments on this manuscript.

Correspondence should be addressed to Dr. Myles H. Akabas, Department of Physiology and Biophysics, Albert Einstein College of Medicine, Bronx, NY 10461. E-mail: makabas@aecom.yu.edu.

DOI:10.1523/JNEUROSCI.0224-06.2006

Copyright © 2006 Society for Neuroscience 0270-6474/06/264492-08\$15.00/0

	... M1		M2		M3					
GABA α ₁	233	PCIMTVILSQ	VSWFLNRESV	PARTVFGVTT	VLT <u>MT</u> TTLSIS	ARNSLPKVAY	AT-AMDWFIA	VCYAFVFSAL	<u>IEFA</u> TVNYFT	310
GABA β ₁	228	PSTLITILSW	VSWWYNDAS	AARVALGITT	VLTMTTISTH	LRETLPKIPY	VK-AIDIYLM	GCFFVFLAL	LEYAFVNYIF	306
GABA γ ₂	243	PCTLIVVLSW	VSWWINKDAV	PARTSLGITT	VLTMTTSTI	ARKSLPKVSY	VT-AMDLFVS	VCFIFVFSAL	VEYGLTHYFV	321
Gly α ₁	230	PSLLIVILSW	ISFWINMDAA	PARVGLGITT	VLTMTTQSSG	SRASLPKVS	VK-AIDIWMA	VCLLFVFSAL	LEYAAVNFVS	308
Gly β ₁	254	PTLLIVVLSW	LSFWINPDAS	AARVPLGIFS	VLSLASECTT	LAAELPKVSY	VK-ALDWVLI	ACLLFGFASL	VEYAVVQVML	332
5HT _{3A}	233	PSIFLVMVDI	VGFCCLPPDSG	-ERVSFKITL	LLGYSVFLII	VSDTLPTATAI	GTPLIGVYFV	VCMALLVISL	AETIFIVQLV	312
5HT _{3B}	223	PSIFLMLVDL	GSFYLPNCR	-ARIVFKTNV	LVGYTVFRVN	MSDEVPRSAG	CTSLIGVFFT	VCMALLVLSL	SKSILLIKFL	302
nACh α ₁	220	PCLLFSFLT	LVFYLPTDSG	-EKMTLSISV	LLSLTVFLLV	IVELIPSTSS	AVPLIGKMYL	FTMVVFIASI	IITVIVINTH	299
nACh β ₁	231	PCILITLLAI	FVFYLPDAG	-EKMGSLIFA	LLTLTVFLLL	LADKVPETSL	AVPIIKIYLM	FTMILVTFV	ILSVVVLNLH	310
nACh δ ₁	234	PCVLISFMIN	LVFYLPGDCG	-EKTSVAISV	LLAQSVFLLL	ISKRLPATSM	AIPLVKGFL	FGMVLVMTV	VICVIVLNH	313
nACh ε ₁	230	PCVLISGLVL	LAYFLPAQAG	GQKCTVSINV	LLAQTVFLFL	IAQKIPETSL	SVPLLLGRYLI	FVMVVATLIV	MNCVIVLNV	309
nACh γ ₁	229	PCVLISVAI	LIYFLPAKAG	GQKCTVATNV	LLAQTVFLFL	VAKKVPETSQ	AVPLISKYLT	FLMVVTILIV	VNSVVVLNV	308
nACh α torma	220	PCLLFSFLT	LVFYLPTDSG	-EKMTLSISV	LLSLTVFLLV	IVELIPSTSS	AVPLIGKMYL	FTMIFVISS	IIVTVVINTH	299
nACh β torma	226	PCILISILAI	LVFYLPPDAG	-EKMSLSISA	LLALTVFLLL	LADKVPETSL	SVPIIISYLM	FIMLVAFVSV	ILSVVVLNLH	305
nACh δ torma	234	PCVLISFLAA	LAFYLPAESG	-EKMTAICV	LLAQAVFLLL	TSQRLPETAL	AVPLIGKMYL	FIMSLVTVGV	VNCGIVLNFH	313
nACh γ torma	228	PCVLISLVV	LVFYLPAQAG	GQKCTLSISV	LLAQTVFLFL	IAQKVPETSL	NVPLIGKMYL	FVMFVSLVIV	TNCVIVLNV	307
		* : : : : . .	:	:: :	:	.* .	:	:: .	:	:

Figure 1. Alignment of GABA_A, Gly, 5-HT₃, and ACh receptor subunit sequences. The lines on top indicate TM regions based on the extents of the TM segments in the 4 Å ACh receptor structure (Unwin, 2005). Residues in the GABA_A α₁ subunit that were mutated in this study are underlined and in bold. The extent of amino acid conservation at each position is indicated below the sequences: absolutely conserved (*), highly conserved (:), and moderately conserved (.). All sequences are the rat sequences except for the bottom four AChR subunits labeled “torma,” which are from *T. marmorata*.

lining face (Xu and Akabas, 1996). In the ACh receptor structure, the aligned residues are in close proximity to M1 and M3, respectively (Miyazawa et al., 2003). Based on the ACh receptor structure, GABA_A M3 residues between α1A300 and α1A305 should lie in close proximity to α1T267. We constructed all of the double cysteine mutants between these M2 and M3 positions and assayed for spontaneous and induced disulfide bond formation in the absence and presence of GABA. Two M3 positions formed disulfide bonds in the closed state but not in the presence of GABA. Disulfide bond formation with a third position in the presence of GABA significantly increased the channels’ spontaneous open probability. These results provide insight into the resting state structure and the conformational motion between M2 and M3 during channel gating in the Cys-loop receptor superfamily.

Materials and Methods

Alignment. Sequences were obtained from UniProt (Universal Protein Resource; <http://www.ebi.uniprot.org/index.shtml>) or RCSB PDB (Research Collaboratory for Structural Bioinformatics; <http://www.rcsb.org/pdb/>), and aligned using ClustalW (<http://www.ebi.ac.uk/clustalw/index.html>). To improve the reliability of the alignment, we performed a multiple alignment with several other members of the Cys-loop superfamily of ligand-gated ion channels.

Mutagenesis and oocyte expression. M2 segment residues can be named using an index numbering system that facilitates comparison between M2 segments of different members of the superfamily. At the cytoplasmic end, the 0’ position is defined as the conserved positively charged residue aligned with GABA_A α1R255, and the 20’ position (Miller, 1989) is the residue aligned with the ACh receptor extracellular ring of charge (Imoto et al., 1988). The rat GABA_A receptor α₁, β₁, and γ_{2S} subunit cDNA constructs in the pGEMHE vector were used. The M2 mutations were introduced using α1 wild-type (wt) or α1M3 single mutants (V297C, A300C, L301C, I302C, E303C, F304C, A305C) as templates (Williams and Akabas, 1999) and the QuikChange mutagenesis kit (Stratagene, La Jolla, CA). Mutational primers (Sigma, St. Louis, MO) introduced M266C (5’-GTG ACG ACC GTT CTG ACC **TGT ACA** ACC TTG AGT ATC AGT GC-3’ and 3’-GCA CTG ATA CTC AAG GTT **GTA CAG** GTC AGA ACG GTC GTC AC-5’) or T267C (5’-ACG ACC GTT CTG ACC ATG **TGT ACA** TTG AGT ATC AGT GCC AG-3’ and 3’-CTG GCA CTG ATA CTC **AAT GTA CAC** ATG GTC AGA ACG GTC GT-5’) and a silent *Bsr*GI site (mutated base pairs in bold; *Bsr*GI recognition site underlined). The identity was verified by restriction digestion and DNA sequencing of the complete coding region. Plasmids were linearized with

*Nhe*I before *in vitro* mRNA transcription with T7 RNA polymerase (Amplicap T7 High Yield Message Maker; Epicenter Technologies, Madison, WI; or mMessage mMachine kit; Ambion, Austin, TX). mRNA was dissolved in diethylpyrocarbamate-treated water and stored at -80°C. Female *Xenopus laevis* were purchased from Nasco Science (Fort Atkinson, WI). Stage V–VI oocytes were defolliculated with a 75 min incubation in 2 mg/ml Type 1A collagenase (Sigma) in OR2 (82.5 mM NaCl, 2 mM KCl, 1 mM MgCl₂, and 5 mM HEPES; pH adjusted to 7.5 with NaOH). Oocytes were washed thoroughly in OR2 and kept in SOS medium (82.5 mM NaCl, 2.5 mM KCl, 1 mM MgCl₂, 5 mM HEPES, pH 7.5) supplemented with 1% antibiotic–antimycotic (100×) liquid (10,000 IU/ml penicillin, 10,000 μg/ml streptomycin, and 25 μg/ml amphotericin B; Invitrogen, Carlsbad, CA) and 5% horse serum (Sigma). Oocytes were injected 24 h after isolation with 50 nl (10 ng) of a 1:1:1 mixture of rat α₁:β₁:γ_{2S} subunit mRNA and were kept in horse serum medium for 2–10 d at 17°C. Mutant subunit mRNA was substituted for wt α₁ subunit where necessary (Horenstein et al., 2001).

Electrophysiology. Electrophysiological recordings were conducted at room temperature in a ~250 μl chamber continuously perfused at a rate of 5–6 ml/min with Ca²⁺-free frog Ringer’s buffer (CFR) (115 mM NaCl, 2.5 mM KCl, 1.8 mM MgCl₂, 10 mM HEPES, pH 7.5 with NaOH) using equipment and procedures described previously (Horenstein and Akabas, 1998). Currents were recorded from individual oocytes using two-electrode voltage-clamp at a holding potential of -60 mV. The ground electrode was connected to the bath via a 3 M KCl/Agar bridge. Glass microelectrodes had a resistance of <2 MΩ when filled with 3 M KCl. Data were acquired and analyzed using a TEV-200 amplifier (Dagan Instruments, Minneapolis, MN), a Digidata 1322A data interface (Molecular Devices, Union City, CA), and pClamp 8 software (Molecular Devices). Currents (*I*_{GABA}) elicited by GABA applications were separated by at least 6 min of CFR wash to allow complete recovery from desensitization. Currents were judged to be stable if the variation between consecutive GABA pulses was ≤10%.

Reagents. GABA (Sigma) was prepared as a 100 mM stock solution in water. Dithiothreitol (DTT) (Sigma) was dissolved in water to obtain a 1 M stock solution and diluted into CFR before each experiment. *o*-Phenanthroline (Sigma) was made as a 1 M stock solution in DMSO and CuSO₄ as a 100 mM stock solution in water. CuSO₄ and *o*-phenanthroline were mixed in CFR before use to a final concentration of 100:200 μM or 10:20 μM Cu:Phen. Tris(2-carboxyethyl)phosphine HCl (TCEP) (Sigma) was dissolved in water to obtain a 100 mM stock and diluted into CFR before each experiment. Picrotoxin was dissolved in DMSO at a 100 mM concentration and diluted in CFR.

DTT effect. Once stable GABA EC₅₀₋₅₀ test currents (*I*) were achieved, 10 mM DTT was applied for 2 min. After a washout period of 6 min the

GABA EC_{30–50} test current was recorded again (I_{DTT}). Potentiation by application of DTT was calculated as follows: effect % = $\{(I_{\text{DTT}} - I) / I_{\text{DTT}}\} \times 100$.

Cu:Phen effect. Oocytes were pretreated with DTT and GABA test pulses (I_{DTT}) were applied. Oocytes were then treated with 100:200 μM Cu:Phen for 2 min, and two more GABA test pulses were applied ($I_{\text{Cu:Phen}}$). A second application of 10 mM DTT for 2 min followed by GABA test pulses was used to test for the reversibility of the Cu:Phen effect. Inhibition by Cu:Phen induced disulfide bonds was calculated as follows: effect % = $\{(I_{\text{Cu:Phen}} - I_{\text{DTT}}) / I_{\text{DTT}}\} \times 100$.

Cu:Phen effect in the presence of GABA, open/desensitized states. For this set of experiments, we first determined the minimum application duration of 10:20 μM Cu:Phen that produces inhibition comparable with a 2 min application of 100:200 μM Cu:Phen. Preliminary experiments with the $\alpha 1\text{T267C}$ L301C double mutant on initially fully reduced (10 mM DTT; 2 min) oocytes using alternating applications of 10:20 μM Cu:Phen for 1 min and GABA EC₃₀ test currents showed that a comparable effect to the application of 100:200 μM Cu:Phen for 2 min was reached after a cumulative exposure to 10:20 μM Cu:Phen of 2 min.

To determine whether disulfide bonds were formed in the open state, we performed the following experiment: Once stable GABA EC_{30–50} test currents (I) were achieved, we applied 10 mM DTT for 2 min. The GABA EC_{30–50} test current was recorded again (I_{DTT}) to determine the extent of spontaneously formed disulfide bonds. After a 20 s GABA EC_{max} pulse, cells were immediately treated with a mixture of the same GABA concentration and 10:20 μM Cu:Phen for 2 min. After washout of the reagents, two more GABA test pulses were applied ($I_{\text{Cu:Phen} + \text{GABA}}$). A second application of 10 mM DTT for 2 min followed by GABA test pulses was used to test for the reversibility of the Cu:Phen effect. Inhibition by disulfide bonds formed in the presence of GABA and Cu:Phen was calculated as follows: effect % = $\{(I_{\text{Cu:Phen} + \text{GABA}} - I_{\text{DTT}}) / I_{\text{DTT}}\} \times 100$.

Cu:Phen induced oxidation was performed for each oocyte in the absence and in the presence of GABA. One-half of the oocytes were first oxidized in the presence and then in the absence of GABA, the other one-half in the reverse order.

Homology modeling. The membrane-spanning domain of the rat GABA_A receptor $\alpha 1$ subunit was modeled on the basis of the 4 Å structure obtained by electron microscopy of crystalline postsynaptic membranes with pentameric ACh receptors of *Torpedo marmorata* [Protein Data Bank (PDB) number 2BG9]. Using Deep View/Swiss Pdb-Viewer, version 3.7 (Guex and Peitsch, 1997; Schwede et al., 2003), we aligned the GABA $\alpha 1$ subunit sequence with the ACh E chain (γ chain) manually, taking the alignment that we obtained with ClustalW, as outlined above, into account. We generated two different models, one without a gap and one with a 1 aa gap in the M2–M3 loop in the GABA $\alpha 1$ sequence compared with the ACh E chain (γ chain) sequence. The ACh structure aligned with the raw sequence was submitted as a modeling request in Swiss Model. The resulting homology modeled $\alpha 1$ structure was subsequently subjected to energy minimization using the GROMOS 43B1 force field *in vacuo* that is part of Swiss-PdbViewer. Figures were rendered with POV-Ray v3.6 (<http://www.povray.org/>) (Bali and Akabas, 2004).

Results

Effect of DTT on wt and mutant 12' Cys receptors

In electrophysiological experiments, we recorded GABA-induced currents (I_{GABA}) from oocytes expressing GABA $\alpha 1\beta 1\gamma 2$ receptors. Where applicable, the $\alpha 1$ wt subunit was substituted by mutant $\alpha 1$ subunits, containing a single engineered Cys in M2 (11' or 12' Cys) or two engineered Cys [one in M2 (11' or 12' Cys) and one in M3]. DTT is a disulfide bond-reducing agent. It contains two sulfhydryl moieties and is thus able to convert protein disulfides to sulfhydryls via a thiol–disulfide exchange reaction. In wt $\alpha 1\beta 1\gamma 2$ receptors, DTT potentiated GABA-induced currents by $14 \pm 4\%$ ($n = 6$) (Fig. 2). Under the same conditions, the single mutant $\alpha 1\text{T267C}$, and the double mutants $\alpha 1\text{T267C-A300C}$, $\alpha 1\text{T267C-I302C}$, $\alpha 1\text{T267C-E303C}$, and $\alpha 1\text{T267C-A305C}$ were not significantly different from wt (one-way

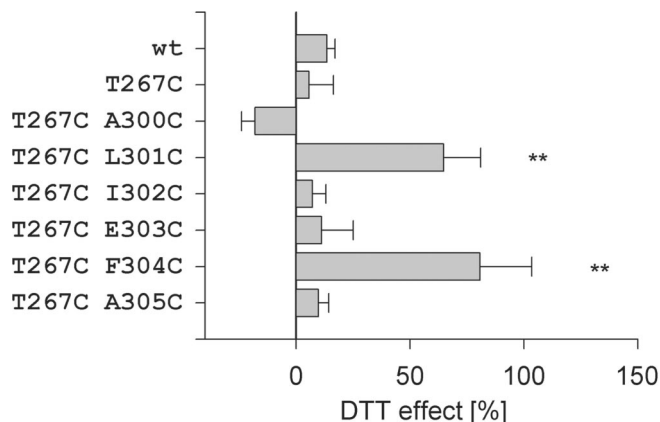


Figure 2. The average effect of a 2 min application of 10 mM DTT on wt and 12' Cys mutants. A positive effect indicates potentiation, and a negative effect indicates inhibition of subsequent GABA-induced currents. The asterisks indicate effects that are significantly different from the effect on wt by a one-way ANOVA, using Dunnett's multiple comparison test, $p < 0.001$. For each condition, the results of three to eight oocytes are averaged. Means \pm SEM are shown.

ANOVA; Dunnett's multiple comparison test; $p > 0.05$). However, the currents in the double mutants $\alpha 1\text{T267C-L301C}$ and $\alpha 1\text{T267C-F304C}$ were potentiated by $71 \pm 25\%$ ($n = 6$) and $81 \pm 32\%$ ($n = 8$), respectively. The potentiation in the double mutants $\alpha 1\text{T267C-L301C}$ and $\alpha 1\text{T267C-F304C}$ was significantly different from wt receptors (one-way ANOVA; Dunnett's multiple comparison test; $p < 0.05$ and $p < 0.01$) (Fig. 2) and may be explained by the reduction of a spontaneously formed disulfide bond between the engineered Cys in M2 and M3. If a disulfide bond were to be formed between these Cys, the relative mobility of at least the M2 and M3 α -helices would be diminished, thus impairing receptor function.

Effect of Cu:Phen on wt and mutant 12' Cys mutants

Under aerobic conditions (oxygen dissolved in CFFR) (with Cu:Phen in a molar ratio of 1:2 serving as a catalyst), oxygen oxidizes the sulfhydryl groups selectively to disulfides but rarely to higher oxidized states (Kobashi, 1968). We tested the effect of Cu:Phen (100:200 μM ; 2 min) on fully reduced wt and 12' Cys single and double mutant receptors. To reduce spontaneously formed disulfide bonds between engineered Cys pairs or between engineered Cys and small endogenous sulfhydryls like cysteine and glutathione, oocytes were first treated with DTT (10 mM; 2 min). Cystine and GSSG (oxidized glutathione) participate in disulfide interchange reactions and are capable of forming mixed disulfides with proteins. After DTT application, oocytes were allowed to equilibrate with CFFR, and GABA pulses were recorded with a frequency of one per 6 min. Subsequently, cells were treated with Cu:Phen (100:200 μM ; 2 min), and after a washout period, the resulting GABA-induced currents were recorded (Fig. 3). There was no effect of oxidation neither in wt receptors, nor the 12' single mutant $\alpha 1\text{T267C}$, nor in the double mutants $\alpha 1\text{T267C-V297C}$, $\alpha 1\text{T267C-A300C}$, $\alpha 1\text{T267C-I302C}$, and $\alpha 1\text{T267C-E303C}$. Cu:Phen inhibited GABA-induced currents in wt, $\alpha 1\text{T267C}$, $\alpha 1\text{T267C-A300C}$, $\alpha 1\text{T267C-I302C}$, and $\alpha 1\text{T267C-E303C}$ by $11 \pm 4\%$ ($n = 6$), $8 \pm 7\%$ ($n = 5$), $3 \pm 4\%$ ($n = 3$), $15 \pm 5\%$ ($n = 5$), $1 \pm 16\%$ ($n = 5$) (one-way ANOVA; $p > 0.05$). However, the double mutants that were potentiated by DTT, namely $\alpha 1\text{T267C-L301C}$ and $\alpha 1\text{T267C-F304C}$, and in addition also $\alpha 1\text{T267C-A305C}$ (Fig. 3E) showed an inhibition of $45 \pm 2\%$ ($n = 18$), $45 \pm 4\%$ ($n = 11$), and $55 \pm 7\%$ ($n = 5$),

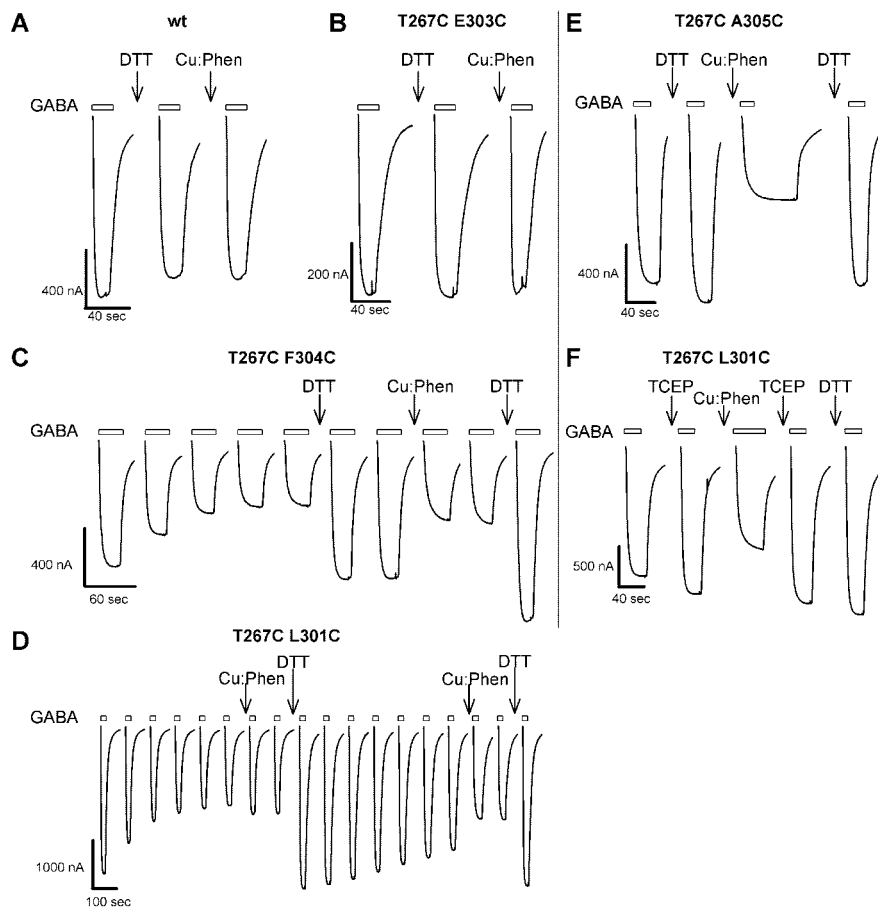


Figure 3. DTT/TCEP and Cu:Phen effect on wt and $\alpha 1$ -12' Cys mutants. GABA-induced current traces before and after 2 min applications of 10 mM DTT or 100:200 μM Cu:Phen from wt and mutant receptors are shown. **A**, Wild-type $\alpha 1\beta 1\gamma 2\delta$ are not significantly affected by either DTT or Cu:Phen. **B**, $\alpha 1\text{T267C-E303C}\beta 1\gamma 2\delta$ are not significantly affected by either DTT or Cu:Phen. **C**, **D**, $\alpha 1\text{T267C-F304C}$ (**C**) and $\alpha 1\text{T267C-L301C}$ (**D**) show spontaneous disulfide bond formation that is reversed by DTT and induced by Cu:Phen. In $\alpha 1\text{T267C-L301C}$ -containing receptors, the current size decreases with each GABA pulse. After reaching a stable plateau, current can be recovered to the initial size after reduction with DTT. A Cu:Phen application inhibits currents to the same extent as reached after repetitive GABA applications. This inhibition is DTT reversible. **E**, In $\alpha 1\text{T267C-A305C}$ -containing receptors, DTT application does not significantly alter the subsequent current. Cu:Phen, however, significantly inhibits these receptors. This inhibition is reversed by DTT application. **F**, $\alpha 1\text{T267C-L301C}$ can be cycled between reduced and oxidized states by reducing with TCEP (1 mM; 2 min) and oxidizing with Cu:Phen (100:200 μM ; 2 min). DTT (10 mM; 2 min) does not significantly potentiate TCEP-treated oocytes. All traces are separated by 6 min washes with CFFR from reagent or GABA applications to allow for washout of excess reagents or complete recovery from desensitization. All GABA current traces represent stable currents: two subsequent GABA currents were not different by $>10\%$. Currents during reagent application are not shown. The bars above the traces indicate the duration of GABA applications; the arrows indicate the application of the indicated reagent.

respectively, that was significantly different from wt (one-way ANOVA; Dunnett's multiple comparison test; $p < 0.001$) (Fig. 4). The Cu:Phen-induced inhibition of GABA currents could be fully reversed by a second application of DTT. The ability to reverse the Cu:Phen inhibition with DTT implies that it is attributable to disulfide bond formation and not attributable to oxidation of one or both of the Cys to a higher-order oxidation state that would not be reducible by DTT. We infer that, by alternatively applying DTT and Cu:Phen, we cycle between fully reduced (free sulfhydryls) and fully oxidized (disulfide-bonded) receptors and that the inhibition in the oxidized state is caused by a disulfide bond that cross-links the engineered Cys in M2 and M3.

Spontaneous formation of disulfide bonds, in the absence of Cu:Phen, was often recorded after GABA applications in the receptors $\alpha 1\text{T267C L301C}$ and $\alpha 1\text{T267C F304C}$ (Fig. 3D). After

stabilization of the current, further oxidation using Cu:Phen (100:200 μM ; 2 min) did not lead to any additional inhibition of GABA-induced currents. Reduction by DTT increased the GABA-induced currents to at least their initial size. In turn, this increase could be reversed by oxidation with Cu:Phen. This spontaneous decrease in the GABA-induced current was not observed in all the oocytes. In some oocytes, the initial current was as big as after DTT application, whereas in others the initial current was as inhibited as after Cu:Phen application. We infer that these differences are attributable to changes in the redox environment of different batches of oocytes, thus leading to varying degrees of spontaneously formed disulfide bonds.

For $\alpha 1\text{T267C-L301C}$ and $\alpha 1\text{T267C-F304C}$, we also determined whether the inhibition by Cu:Phen (100:200 μM ; 2 min) could be reversed by application of TCEP (Fig. 3E). TCEP is a reducing agent that, contrary to DTT, forms only weak complexes with heavy metals (Krezel et al., 2003). Thus, if after TCEP application GABA-induced currents are potentiated, this can only be caused by reduction of disulfide bonds and not by chelating heavy metals. After a 2 min Cu:Phen application (100:200 μM), $\alpha 1\text{T267C-A301C}$ receptors were inhibited by $52 \pm 2\%$ ($n = 3$) and $\alpha 1\text{T267C-F304C}$ receptors by $60 \pm 2\%$ ($n = 5$). This inhibition could be reversed by a 1 min treatment with 2 mM TCEP. A subsequent application of DTT did not potentiate GABA currents any further ($\alpha 1\text{T267C-A301C}$: $0 \pm 5\%$, $n = 3$; $\alpha 1\text{T267C-F304C}$: $-7 \pm 2\%$, $n = 5$). We infer that both the $\alpha 1\text{T267C-A301C}$ and the $\alpha 1\text{T267C-F304C}$ disulfide bond are accessible for both the smaller and membrane-permeant DTT and for the larger and triple negatively charged, and thus membrane-impermeant, TCEP.

Cu:Phen effect on the 12' mutants $\alpha 1\text{T267C-L301C}$, $\alpha 1\text{T267C-F304C}$, and $\alpha 1\text{T267C-A305C}$ in the absence and presence of GABA

In the absence of GABA, the channels are primarily in the closed, unliganded state. In the presence of GABA, the channels undergo rapid transitions between the open, desensitized and closed states. In addition, there are multiple open and desensitized states. Given the timescale of the transitions (milliseconds) and the timescale of the experiments (tens of seconds), we cannot distinguish in which state disulfide bond formation is occurring in the presence of GABA.

We examined the effect of agonist coapplication on Cu:Phen-induced disulfide bond formation. The effect of 10:20 μM Cu:Phen on $\alpha 1\text{T267C-L301C}$ and $\alpha 1\text{T267C-F304C}$ containing receptors was abolished when it was coapplied with GABA. The

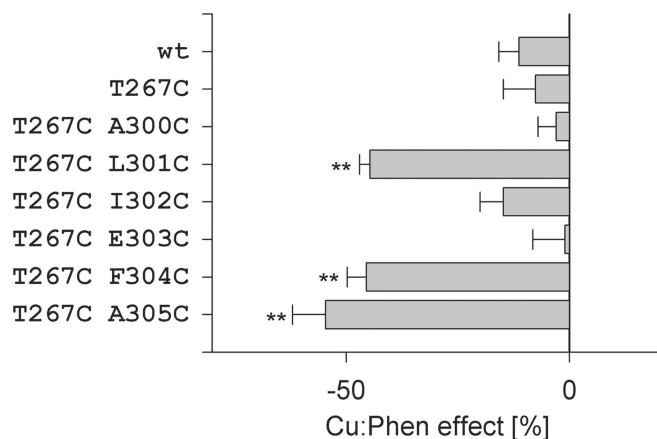


Figure 4. The average effect of a 2 min application of 100:200 μM Cu:Phen on wt and 12' Cys mutants. A positive effect indicates potentiation, and a negative effect indicates inhibition of subsequent GABA-induced currents. The asterisks indicate effects that are significantly different from the effect on wt by a one-way ANOVA, using Dunnett's multiple comparison test, $p < 0.001$. For each condition, the results of 3–18 oocytes are averaged. Means \pm SEM are shown.

double mutant $\alpha\text{T267C-L301C}$ was inhibited by $36 \pm 2\%$ ($n = 4$) by applying Cu:Phen (10:20 μM ; 2 min) alone compared with $7 \pm 4\%$ ($n = 4$) by applying Cu:Phen (10:20 μM ; 2 min) in the presence of a saturating GABA concentration. When compared with a paired t test, the effect in the closed state is significantly different from the one in the open state ($p = 0.015$). The $\alpha\text{T267C-F304C}$ receptors were inhibited by $31 \pm 1\%$ ($n = 4$) by applying Cu:Phen alone and by $-12 \pm 6\%$ ($n = 4$) by applying Cu:Phen together with GABA (paired t test; $p = 0.0057$). The propensity to form a disulfide bond in the closed state is increased for $\alpha\text{T267C-L301C}$ and $\alpha\text{T267C-F304C}$.

In contrast to these two double mutants, the amount of inhibition of the GABA peak currents for the $\alpha\text{T267C-A305C}$ mutant increased from $26 \pm 3\%$ ($n = 4$) with Cu:Phen alone to $67 \pm 6\%$ ($n = 4$) for Cu:Phen in the presence of GABA (paired t test; $p = 0.0012$). We conclude that the distance/relative orientation of the 12' Cys in M2 and the 305Cys in M3 is different in the closed (absence of GABA) and open/desensitized (presence of GABA) states. In the double mutant, $\alpha\text{T267C-A305C}$, a significant change in leak current was induced by coapplication of Cu:Phen with GABA, but not by Cu:Phen alone (Fig. 5C). Subsequent treatment with DTT reversed both the increase in leak current and also the decrease in GABA-induced current amplitude. The increase in leak current could be transiently blocked by applying the open channel blocker picrotoxin (50 μM) (Fig. 5D). We infer that, when $\alpha\text{T267C-A305C}$ is oxidized in the open state, the receptor is trapped in a conformation for which the spontaneous open probability is increased. Therefore, the current amplitude that can result from GABA application is decreased. If the increase in leak current after a combined GABA-Cu:Phen application is added to the GABA current amplitude after the Cu:Phen plus GABA application, the inhibition would be $24 \pm 7\%$ ($n = 4$), which is comparable with the inhibition caused by application of Cu:Phen alone.

Effect of DTT and Cu:Phen on $\alpha\text{T267C-V297C}$

We sought to test the extent of vertical motion of M3 relative to the 12' M2 position. V297 lies on the same face of the M3 helix as the reactive residues but one helical turn closer to the extracellular side. Application of 10 mM DTT for 2 min or 100:200 μM Cu:Phen for 2 min had no effect on the GABA-induced currents

of the double mutant $\alpha\text{T267C-V297C}$. We infer that a disulfide bond does not form between these two residues, implying that there is limited vertical motion of the M3 segment relative to the M2 segment.

Cu:Phen effect on the 11' mutants $\alpha\text{1M266C-L301C}$, $\alpha\text{1M266C-F304C}$, and $\alpha\text{1M266C-A305C}$ in the absence and presence of GABA

As a control for possible reaction of the M3 Cys with endogenous cysteines, we tested the effects of DTT and Cu:Phen on the redox-sensitive M3 Cys mutants in the presence of the 11' Cys mutant α1M266C . A 2 min application of 10 mM DTT had no significant effects on the subsequent GABA-induced currents in oocytes expressing the mutants α1M266C , $\alpha\text{1M266C-L301C}$, $\alpha\text{1M266C-F304C}$, or $\alpha\text{1M266C-A305C}$ compared with wild type (one-way ANOVA with Dunnett's multiple comparison test; $p > 0.05$) (data not shown). We infer that no disulfide bonds formed spontaneously between these pairs of Cys mutants or between these Cys mutants and the endogenous cysteines.

We also tested the effect of oxidation on these mutants with a 2 min application of 100:200 μM Cu:Phen to oocytes expressing these mutants in the absence and presence of GABA. There was no significant effect on the subsequent GABA-induced currents compared with wild type (one-way ANOVA with Dunnett's multiple comparison test; $p > 0.05$) (data not shown). We infer that disulfide bonds were not formed between the M2–11' Cys and these M3 residues. Furthermore, we infer that these M3 Cys mutants did not form disulfide bonds with endogenous cysteine residues. Thus, we conclude that the effects described in the previous sections with the double Cys mutants containing the M2–12' Cys arose because of disulfide bond formation between the M2–12' Cys and the corresponding M3 Cys.

Homology modeling

The first step in constructing a homology model is to align the respective sequences. As noted in Introduction, this is easy for ACh and GABA_AM1 and M2 segments because of the presence of a series of absolutely conserved residues (Fig. 1). Alignment of the M3 segments is more difficult. Depending on the number of sequences analyzed by multiple sequence alignment programs, either no gap or a one residue gap is created in the M2–M3 loop of the GABA_A receptor sequences compared with the AChR sequences. Having identified the GABA_A α1M3 residues that are in close proximity to $\alpha\text{1M2-12'}$ as L301, F304, and A305, we can conclude that these residues should align with AChR residues in close proximity to $\alpha\text{M2-12'}$ in the AChR structure (Unwin, 2005). These residues are ACh M3 αI289 , αT292 , and αV293 . These residues align with the GABA_A receptor M3 residues that we identified if one assumes a one residue gap in the M2–M3 loop as shown in Figure 1.

We constructed homology models (see Materials and Methods) with no or one residue gaps in the M2–M3 loop (Fig. 6, compare *A*, *B*). The channel-lining M2 residues are in good agreement with our previous substituted cysteine accessibility results (Xu and Akabas, 1993, 1996). The lack of the 1 aa gap in the M2–M3 loop introduces a 100° rotation of the M3 segment residues. Consequently, the face of M3 that apposes M2 is made up of different amino acids in both models. Based on our cross-linking results, we infer that the alignment with the 1 aa gap in the M2–M3 loop must be used to thread the GABA_A receptor α1 subunit onto the AChR structure. This suggests that the M2–M3 loop is one residue shorter in the GABA_A receptor compared with

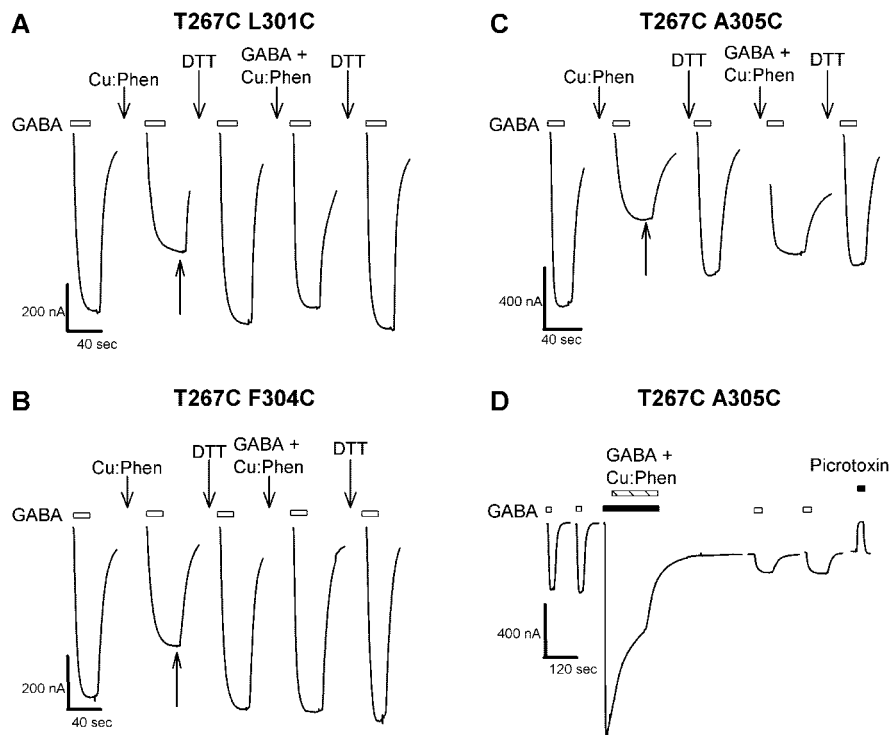


Figure 5. Effect of a 2 min application of 10:20 μM Cu:Phen applied in the presence or in the absence of GABA on GABA-induced currents from oocytes expressing 12' Cys mutants. **A, B**, In $\alpha 1\text{T}267\text{C-L}301\text{C}$ (**A**)- and in $\alpha 1\text{T}267\text{C-F}304\text{C}$ (**B**)-containing receptors, a 2 min application of Cu:Phen in the absence of GABA inhibited the subsequent GABA currents. This inhibition was reversed by DTT. A subsequent 2 min application of Cu:Phen in the presence of EC_{80} GABA did not inhibit the subsequent GABA currents. An additional DTT application did not change the current size. Reagents were applied at the downward arrows. Currents are not shown during reagent applications. **C**, In $\alpha 1\text{T}267\text{C-A}305\text{C}$ receptors, a 2 min application of Cu:Phen in the absence of GABA inhibited the subsequent GABA current. Reduction with DTT reversed the inhibition of the GABA current. A subsequent 2 min application of Cu:Phen in the presence of GABA had two effects on the following GABA currents. A large increase in the holding current was observed (note the level at which the subsequent GABA current begins), and the magnitude of the subsequent GABA current was significantly reduced. It is notable that the magnitude of the total current, the sum of the holding current and the GABA-induced current, was similar to the GABA current before the Cu:Phen/GABA application. The increased holding current and the reduced GABA current were reversed by a subsequent reduction with DTT. **D**, Currents from an oocyte expressing $\alpha 1\text{T}267\text{C-A}305\text{C}$. Application and washout of Cu:Phen in the presence of GABA caused a significant increase in the holding current and a reduction in the GABA test current. The increased holding current was inhibited by application of 50 μM picrotoxin. All GABA current traces represent stable currents: two subsequent GABA currents were not different by $>10\%$. Only one is shown for the sake of clarity. Currents during reagent application are not shown. The bars above the traces indicate the duration of application of GABA; the arrows indicate the application of the given reagent.

the ACh and 5-HT₃ receptor subunits. The functional consequences of this remain to be investigated.

Discussion

These results have important implications for Cys-loop receptor structure–function. First, the closed state disulfide bonds provide an experimental basis for alignment of GABA_A and ACh M3 segments, an essential step to constructing realistic GABA_A homology models based on the 4 Å AChR structure. This will provide a molecular framework for interpreting the effects of GABA_A mutations on general anesthetic efficacy. Second, disulfide bond formation in the presence of GABA that increases spontaneous channel opening may provide insight into the conformational changes that M2 channel-lining segments undergo during channel opening in GABA_A and other Cys-loop receptors.

Homology modeling offers the possibility of applying to GABA_A receptors the recent advances in our understanding of ACh receptor structure. It is, however, essential to align correctly the ACh and GABA_A sequences. In the transmembrane domain, absolutely conserved residues in and flanking M1 and M2 facili-

tate correct alignment but depending on the number of sequences aligned, multiple sequence alignment programs introduce a gap in the M2–M3 loop (Fig. 1). This, coupled with the low sequence identity in M3, makes it difficult to align the ACh and GABA_A M3 segments. We used an unbiased search to determine the proximity between M2 and M3 residues. In the closed state, disulfide bonds formed spontaneously between M2–12', $\alpha 1\text{T}267\text{C}$, and both M3 $\alpha 1\text{L}301\text{C}$ and $\alpha 1\text{F}304\text{C}$ and could be induced with $\alpha 1\text{A}305\text{C}$. These three residues lie on one face of the M3 helix. In the closed state, this face of M3 lies in close proximity to M2 (Fig. 6). When the M2 Cys was moved to the adjacent position $\alpha 1\text{M}266\text{C}$ (11'), which should face M1, oxidation had no effect on any of these M3–Cys mutants, confirming the specificity of the reaction between M2–12' Cys and these M3 cysteines. In our homology model, based on the AChR structure (Unwin, 2005), the M2–12' α carbon is within 10 Å of the α carbons of these three M3 residues (Fig. 6). In a disulfide bond, the α carbons can be separated by at most 5.6 Å (Careaga and Falke, 1992). This implies that 4–5 Å relative movements of M2 and M3 would bring these positions into sufficiently close proximity to permit disulfide bond formation. Previously, we showed that M2 undergoes even larger translational movements at the 20' level (Horenstein et al., 2005) that are facilitated by the loose protein packing around the extracellular one-half of M2 (Goren et al., 2004; Unwin, 2005). Because disulfide bonds formed spontaneously with L301C and F304C, we infer that the collision frequency of M2–12' with these positions was higher and/or the orientation was more favorable than with A305C (Fig. 6C–E,G). In the *Torpedo* AChR structure, the α subunit M3 residues in close proximity to M2–12' are I289, T292, and V293 (Unwin, 2005). To align these ACh and GABA_A residues, a single gap must be introduced into the M2–M3 loop (Figs. 1, 6). Thus, despite the cogent rationale offered recently for a two residue gap in the M2–M3 loop (Ernst et al., 2005), it is not supported by our current experiments. Furthermore, our results imply that the relative depths of the M2 and M3 segments in the 2BG9 AChR structure are correct (Unwin, 2005).

Our results place limits on the extent of thermal motion occurring in this region of M3. The absence of disulfide bond formation with residues on the backside of M3 implies that M3 does not undergo significant rotational motion in the closed state. The absence of disulfide bond formation between M2–12'C and M3–V297C, the residue on the reactive face one helical turn more extracellular than L301, implies that in the closed state the upward displacement (i.e., perpendicular to the membrane plane) of M2 relative to M3 is less than ~ 5 Å. The α -carbon separation between M2–12' and V297 is 10 Å (Fig. 6G). Furthermore, $\alpha 1\text{Cys}293$, an endogenous cysteine on the same helical face one

turn above V297 (Fig. 6G), did not form a disulfide bond with the M2–12' Cys because neither DTT nor Cu:Phen had any effect on the single M2–12' Cys mutant. These results, combined with the lack of reaction of sulfhydryl-reactive reagents with M3 engineered Cys residues below α 1Y294C in the closed state (Williams and Akabas, 1999) suggest that M3 has limited thermal motion and water surface accessibility in the closed state. In contrast, M2 undergoes significant thermal motion in the closed state, particularly above 12' (Horenstein et al., 2001; Bera and Akabas, 2005; Horenstein et al., 2005). These results also place limits on the potential rotational movement of M2, because no disulfide bonds formed between the M2–11' position and any of the M3 Cys mutants.

GABA activation altered the orientation and/or relative position of M2 and M3. Previously, we showed that GABA activation increased the water accessibility of several M3 positions including L301, suggesting that M3 and/or its surroundings underwent a conformational change during gating (Williams and Akabas, 1999). With GABA, disulfide bonds did not form or formed at a significantly slower rate between M2–12'C and either L301C or F304C (Fig. 5A,B). In contrast, an α 1T267C-A305C disulfide bond formed in the presence and absence of GABA, but the functional effect was quite different: When induced in the absence of GABA, the subsequent GABA currents were inhibited, whereas in the presence of GABA, it caused a significant increase in the spontaneous open probability that was inhibited by picrotoxin and reversed by DTT (Fig. 5C,D). We infer that, in the closed and activated states, disulfide bond formation trapped the receptor in two distinct conformations that were not interchangeable after bond formation. This conformational change could involve an \sim 5 Å translational movement of M2 toward the M1 segment in the counterclockwise adjacent subunit (looking from the extracellular side).

How could an α 1T267C-A305C disulfide bond increase spontaneous opening? In the closed state, the M2 segments probably fluctuate continuously between their closed and open conformations, although predominantly in the closed conformation. Presumably, spontaneous opening and ion conduction only occurs when all five M2 segments are in the open conformation, which rarely occurs in the absence of GABA. We infer that the α 1T267C-A305C disulfide bond formed in the presence of GABA holds the two α 1M2 segments in a conformation similar to their open conformation. Thus, after disulfide bond formation, spontaneous opening would only require the remaining three M2 segments to simultaneously enter the open conformation. This would significantly increase the spontaneous open probability. Alternatively, the conformation with the α subunit disulfide

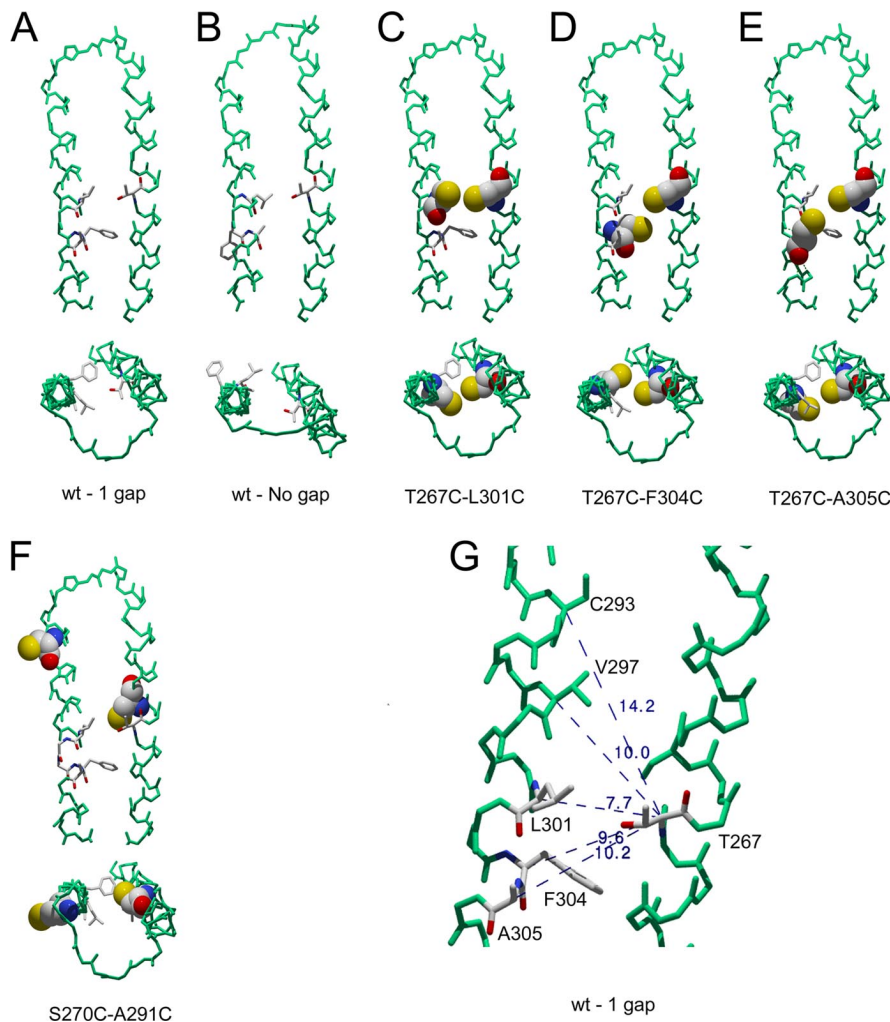


Figure 6. Homology model. A homology model of the GABA_A receptor α 1 subunit was generated using the nicotinic ACh receptor structure (PDB number 2BG9) as a template. The M2 and M3 helices and the connecting M2–M3 loop are shown in wireframe representation (green). Positions at which disulfide bonds formed are shown in CPK colors. In **A–F**, two views of the M2 and M3 segments of wt and mutant receptors are shown from the side (top) and top (bottom). **A** shows a model with a 1 aa gap in the M2–M3 loop; note the proximity of the M3 positions that formed disulfide bonds with the M2–12' position. M2 is on the right. **B** shows the same residues in a model with no gap in the M2–M3 loop. Note that the residues that formed disulfide bonds are not in close proximity in this model. **C–G** were generated using the model containing a single gap in the M2–M3 loop as shown in **A**. **C–E** illustrate the proximity of the pairs of residues that formed disulfide bonds. van der Waals surfaces of Cys substituted at these positions are shown. **F**, Mutations at M2–15' S270 and M3 A291 alter the action of general anesthetics. van der Waals surfaces of Cys substituted at these positions are shown. The α carbons are separated by \sim 15 Å, making it unlikely that they are part of a single binding site. **G** shows the α -carbon separation of the M2–12' residue and several M3 residues.

bonds might induce a conformational change in the M2 segments of the neighboring subunits. We cannot distinguish between these possibilities, although we favor the former. Previously, we found that spontaneous channel opening increased when a disulfide bond formed in the presence of GABA between M2–6' Cys in adjacent subunits (Horenstein et al., 2001). Thus, there are multiple positions where disulfide bond formation in the GABA-activated state leads to increased spontaneous channel opening. These may provide insight into the conformational changes that occur during channel activation.

GABA_A M2–15' mutations alter general anesthetic potentiation in both heterologous expression systems and knock-in mice (Belelli et al., 1997; Mihic et al., 1997; Jurd et al., 2003). Mutations of residues aligned with M3- α 1A291 also alter general anesthetic potentiation (Mihic et al., 1997; Krasowski et al., 2001; Bali and Akabas, 2004). These two positions were widely assumed to be

part of a single anesthetic binding site; however, the intravenous anesthetic propofol only protected a Cys at the β 2M3 site from modification by sulfhydryl reagent, suggesting that they were separate sites (Bali and Akabas, 2004). Using unrelated four-helix-bundle proteins as templates, models were constructed that placed these two positions in close proximity (Trudell and Bertaccini, 2002). Other investigators, using the effects of Hg²⁺ on Cys mutants substituted at the aligned positions in glycine receptors, concluded that a single Hg²⁺ ion could bind simultaneously to engineered Cys at both positions (Lobo et al., 2004). In our homology model, based on the 2BG9 coordinates and our current results, the α carbons of α 1M2–15' and M3– α 1A291 are separated by 15.6 Å (Fig. 6F). This suggests that they are not part of a single binding site. The lack of rotation of M3 and the limited vertical movement make it unlikely that thermal motion could bring these positions into close proximity. Given their separation, we doubt that a single Hg²⁺ could simultaneously bind to Cys at both sites (Lobo et al., 2004). More likely, each Cys bound separate Hg²⁺ ions leading to the reported effects.

Our results provide experimental evidence for the correct threading of the GABA_A M3 segment onto the AChR structure. They support the ClustalW sequence alignment with a one residue gap in the GABA_A and glycine M2–M3 loops compared with the ACh and 5-HT₃ receptors. How this alters interactions between this loop and the extracellular domain that are critical for channel gating (Kash et al., 2003; Lummis et al., 2005; Reeves et al., 2005) remain to be elucidated. The development of more realistic GABA_A receptor homology models will lead to a better understanding of general anesthetic binding and of the conformational changes induced by agonist activation and by anesthetics.

References

- Bali M, Akabas MH (2004) Defining the propofol binding site location on the GABA_A receptor. *Mol Pharmacol* 65:68–76.
- Belelli D, Lambert JJ, Peters JA, Wafford K, Whiting PJ (1997) The interaction of the general anesthetic etomidate with the gamma-aminobutyric acid type A receptor is influenced by a single amino acid. *Proc Natl Acad Sci USA* 94:11031–11036.
- Bera AK, Akabas MH (2005) Spontaneous thermal motion of the GABA(A) receptor M2 channel-lining segments. *J Biol Chem* 280:35506–35512.
- Brejč K, van Dijk WJ, Klaassen RV, Schuurmans M, van Der Oost J, Smit AB, Sixma TK (2001) Crystal structure of an ACh-binding protein reveals the ligand-binding domain of nicotinic receptors. *Nature* 411:269–276.
- Careaga CL, Falke JJ (1992) Thermal motions of surface alpha-helices in the D-galactose chemosensory receptor. Detection by disulfide trapping. *J Mol Biol* 226:1219–1235.
- Celie PH, van Rossum-Fikkert SE, van Dijk WJ, Brejč K, Smit AB, Sixma TK (2004) Nicotine and carbamylcholine binding to nicotinic acetylcholine receptors as studied in AChBP crystal structures. *Neuron* 41:907–914.
- Cromer BA, Morton CJ, Parker MW (2002) Anxiety over GABA(A) receptor structure relieved by AChBP. *Trends Biochem Sci* 27:280–287.
- Ernst M, Bruckner S, Boriesch S, Sieghart W (2005) Comparative models of GABA_A receptor extracellular and transmembrane domains: important insights in pharmacology and function. *Mol Pharmacol* 68:1291–1300.
- Goren EN, Reeves DC, Akabas MH (2004) Loose protein packing around the extracellular half of the GABA_A receptor β 1 subunit M2 channel-lining segment. *J Biol Chem* 279:11198–11205.
- Guex N, Peitsch MC (1997) SWISS-MODEL and the Swiss-PdbViewer: an environment for comparative protein modeling. *Electrophoresis* 18:2714–2723.
- Hevers W, Lüddens H (1998) The diversity of GABA_A receptors. Pharmacological and electrophysiological properties of GABA_A channel subtypes. *Mol Neurobiol* 18:35–86.
- Horenstein J, Akabas MH (1998) Location of a high affinity Zn²⁺ binding site in the channel of alpha1beta1 gamma-aminobutyric acid A receptors. *Mol Pharmacol* 53:870–877.
- Horenstein J, Wagner DA, Czajkowski C, Akabas MH (2001) Protein mobility and GABA-induced conformational changes in GABA_A receptor pore-lining M2 segment. *Nat Neurosci* 4:477–485.
- Horenstein J, Riegelhaupt P, Akabas MH (2005) Differential protein mobility of the gamma-aminobutyric acid, type A, receptor alpha and beta subunit channel-lining segments. *J Biol Chem* 280:1573–1581.
- Imoto K, Busch C, Sakmann B, Mishina M, Konno T, Nakai J, Bujo H, Mori Y, Fukuda K, Numa S (1988) Rings of negatively charged amino acids determine the acetylcholine receptor channel conductance. *Nature* 335:645–648.
- Jurd R, Arras M, Lambert S, Drexler B, Siegwart R, Crestani F, Zaugg M, Vogt KE, Ledermann B, Antkowiak B, Rudolph U (2003) General anesthetic actions in vivo strongly attenuated by a point mutation in the GABA(A) receptor beta3 subunit. *FASEB J* 17:250–252.
- Karlin A (2002) Emerging structure of the nicotinic acetylcholine receptors. *Nat Rev Neurosci* 3:102–114.
- Kash TL, Jenkins A, Kelley JC, Trudell JR, Harrison NL (2003) Coupling of agonist binding to channel gating in the GABA(A) receptor. *Nature* 421:272–275.
- Kobashi K (1968) Catalytic oxidation of sulfhydryl groups by o-phenanthroline copper complex. *Biochim Biophys Acta* 158:239–245.
- Krasowski MD, Nishikawa K, Nikolaeva N, Lin A, Harrison NL (2001) Methionine 286 in transmembrane domain 3 of the GABA_A receptor beta subunit controls a binding cavity for propofol and other alkylphenol general anesthetics. *Neuropharmacology* 41:952–964.
- Krezel A, Latajka R, Bujacz GD, Bal W (2003) Coordination properties of tris(2-carboxyethyl)phosphine, a newly introduced thiol reductant, and its oxide. *Inorg Chem* 42:1994–2003.
- Le Novère N, Changeux JP (1999) The ligand gated ion channel database. *Nucleic Acids Res* 27:340–342.
- Lester HA, Dibas MI, Dahan DS, Leite JF, Dougherty DA (2004) Cys-loop receptors: new twists and turns. *Trends Neurosci* 27:329–336.
- Lobo IA, Trudell JR, Harris RA (2004) Cross-linking of glycine receptor transmembrane segments two and three alters coupling of ligand binding with channel opening. *J Neurochem* 90:962–969.
- Lummis SC, Beene DL, Lee LW, Lester HA, Broadhurst RW, Dougherty DA (2005) Cis-trans isomerization at a proline opens the pore of a neurotransmitter-gated ion channel. *Nature* 438:248–252.
- Mihic SJ, Ye Q, Wick MJ, Koltchine VV, Krasowski MD, Finn SE, Mascia MP, Valenzuela CF, Hanson KK, Greenblatt EP, Harris RA, Harrison NL (1997) Sites of alcohol and volatile anaesthetic action on GABA(A) and glycine receptors. *Nature* 389:385–389.
- Miller C (1989) Genetic manipulation of ion channels: a new approach to structure and mechanism. *Neuron* 2:1195–1205.
- Miyazawa A, Fujiyoshi Y, Unwin N (2003) Structure and gating mechanism of the acetylcholine receptor pore. *Nature* 423:949–955.
- Reeves DC, Jansen M, Bali M, Lemster T, Akabas MH (2005) A role for the β 1– β 2 loop in the gating of 5-HT₃ receptors. *J Neurosci* 25:9358–9366.
- Schwede T, Kopp J, Guex N, Peitsch MC (2003) SWISS-MODEL: an automated protein homology-modeling server. *Nucleic Acids Res* 31:3381–3385.
- Trudell JR, Bertaccini E (2002) Molecular modelling of specific and non-specific anaesthetic interactions. *Br J Anaesth* 89:32–40.
- Trudell JR, Bertaccini E (2004) Comparative modeling of a GABA_A alpha1 receptor using three crystal structures as templates. *J Mol Graph Model* 23:39–49.
- Unwin N (2005) Refined structure of the nicotinic acetylcholine receptor at 4Å resolution. *J Mol Biol* 346:967–989.
- Williams DB, Akabas MH (1999) Gamma-aminobutyric acid increases the water accessibility of M3 membrane-spanning segment residues in gamma-aminobutyric acid type A receptors. *Biophys J* 77:2563–2574.
- Xu M, Akabas MH (1993) Amino acids lining the channel of the gamma-aminobutyric acid type A receptor identified by cysteine substitution. *J Biol Chem* 268:21505–21508.
- Xu M, Akabas MH (1996) Identification of channel-lining residues in the M2 membrane-spanning segment of the GABA_A receptor alpha1 subunit. *J Gen Physiol* 107:195–205.